RSC Advances

PAPER

View Article Online
View Journal | View Issue

Cite this: *RSC Adv.*, 2022, **12**, 4697

Facile synthesis of peanut-like Sn-doped silica nano-adsorbent for affinity separation of proteins

Mochou Gao,[ae] Qin Liu,[bdf] Yuanyuan Xue,[bdf] Bao Li,[abd] Xingchi Liu,[abd] Zhenzhu Shi,[bdf] Nan Liu*[f] and Xueyan Zou *[acd]

A peanut-like hollow silica (denoted as p-l-$hSiO_2$) adsorbent is prepared in a facile method, which is composed of several silica nanospheres and has an average diameter of 22 nm, with thickness of 5 nm. Its Brunauer–Emmett–Teller (BET) surface area, pore volume and pore size are 258.9 m^2 g^{-1}, 1.56 cm^3 g^{-1} and 3.9 nm, respectively. Then the afforded p-l-$hSiO_2$/GSH adsorbent is applied to purify glutathione S-transferases-tagged (denoted as GST-tagged) proteins. It is found that the p-l-$hSiO_2$ adsorbent exhibits a specific adsorption, a high binding capacity (6.80 mg g^{-1}), good recycling performance and high recovery (90.1%) to the target proteins, showing promising potential for the affinity separation of GST-tagged proteins.

Received 15th November 2021
Accepted 25th January 2022

DOI: 10.1039/d1ra08362g

rsc.li/rsc-advances

Introduction

The separation and purification of proteins is an important topic in the field of proteomics.[1–5] Traditional protein isolation and purification methods are usually highly selective for the target protein, however, these methods require multi-step processes such as precipitation, dialysis, filtration, and chromatography.[6–8] These processes are complex, time-consuming, and costly to process. With the development of biology, proteins can be expressed with certain tags, so that proteins can be specifically separated and purified by this tag.[9–13] Glutathione S-transferases (GST) are a multigene family of detoxification enzymes that protect the body against chemical carcinogenesis as well as a family of multifunctional dimeric proteins that can conjugate reduced glutathione with a wide range of electrophilic substrates. Therefore, it is significant to separate and purify GST-tagged proteins for molecular immunology as well as structural, biochemical and cell biological studies.

Affinity chromatography is currently available for the separation and purification of GST-tagged proteins.[14–18] However, this method needs pretreatment and requires long operation time as well as good solubility of the proteins, which limits its application in engineering. These drawbacks, fortunately, can be overcome by applying nanomaterials to assist the affinity separation of the target proteins.[19–23] For example, bio-functionalized silica nanospheres (NSs) can be employed to realize specific separation of GST,[24] and several iron oxide nanoparticles can be applied to well separate His-tagged proteins.[25] The separation efficiency of these inorganic nanoparticles (NPs) towards the proteins, unfortunately, is degraded by their limited surface area and low –GSH group density.

To break the bottleneck, we draw special attention to silica hollow nanospheres, because they may have much larger specific surface area and can greatly increase separation efficiency towards the target proteins than conventional silica NPs.[26] In this research, therefore, we prepare peanut-like glutathione-functionalized silica hollow NSs (denoted as p-l-$hSiO_2$ adsorbent), which are composed of several hollow silica NSs by doped Sn bridge. The prepared p-l-$hSiO_2$ adsorbent has a bigger BET surface aera. Then the GSH group can be modified on the surface of the adsorbent. Finally, GST-tagged proteins were purified from *E. coli* lysate with the prepared p-l-$hSiO_2$ adsorbent with a high capacity.

Results and discussion

Fig. 1a and b shows the SEM and TEM images of the synthesized samples. It can be seen that the prepared sample is hollow spheres, which is about 22 nm in size (Fig. 1a and b). Interestingly, when SnO_2 QDs is added in the solution, the gotten p-l-$hSiO_2$ sample is of a peanut-like shape and consisted of several silica hollow nanospheres with an average diameter of 20 nm and thickness of 5 nm (Fig. 1c and d). Meanwhile, the p-l-$hSiO_2$–GSH sample shows the same peanut-like shape (Fig. 1e and f), meaning there is little effect on the morphology of the sample.

[a]*Engineering Research Center for Nanomaterials, Henan University, Kaifeng 475004, China. E-mail: zouxueyan@henu.edu.cn; 13688869875@163.com*
[b]*College of Chemistry and Chemical Engineering, Henan University, Kaifeng 475004, China*
[c]*Henan Ding You Agriculture Science and Technology Co., LTD., Zhengzhou 450047, China*
[d]*State Key Laboratory of Cotton Biology, Kaifeng 475004, China*
[e]*National & Local Joint Engineering Research Center for Applied Technology of Hybrid Nanomaterials, Kaifeng 475004, China*
[f]*Key Laboratory for Monitor and Remediation of Heavy Metal Polluted Soils of Henan Province, Jiyuan 459000, China*

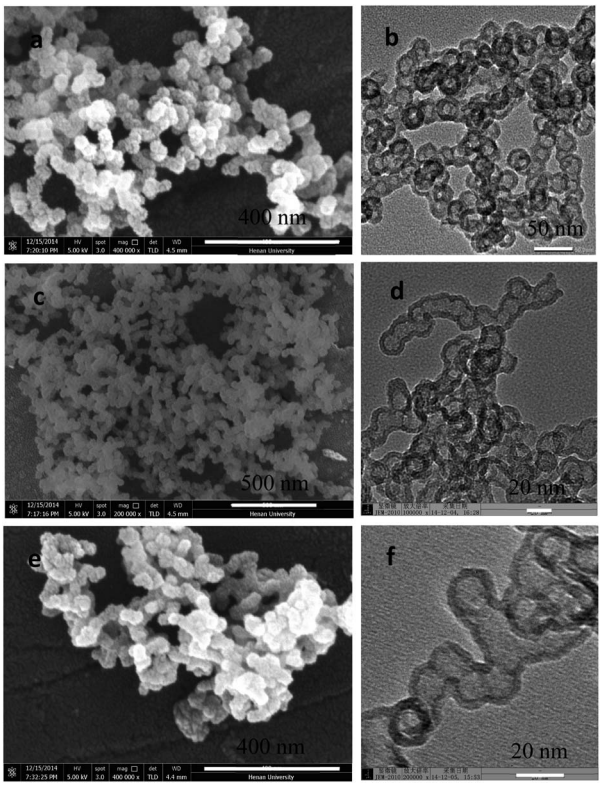

Fig. 1 SEM (a, c and e) and TEM (b, d and f) images of prepared samples. (a and b) Hollow silica without SnO_2; (c and d) p-l-hSiO_2; (e and f) p-l-hSiO_2–SH.

Fig. 2a and c display the nitrogen adsorption–desorption isotherms of the prepared hollow SiO_2 and p-l-hSiO_2 samples. From Fig. 2a, it can be seen that the BET surface area, pore volume and pore size are 122.5 m^2 g^{-1}, 0.27 cm^3 g^{-1}, and 1.5 nm, respectively. Compared with hollow SiO_2, the gotten p-l-hSiO_2 sample has a bigger BET surface area (258.9 m^2 g^{-1}) and pore size (3.9 nm). Fig. 2b and d displays the pore size distribution of the prepared hollow SiO_2 and p-l-hSiO_2 samples. It can be seen that both the hollow SiO_2 and p-l-hSiO_2 have typical type IV adsorption isotherm with a distinct hysteresis loop.[27]

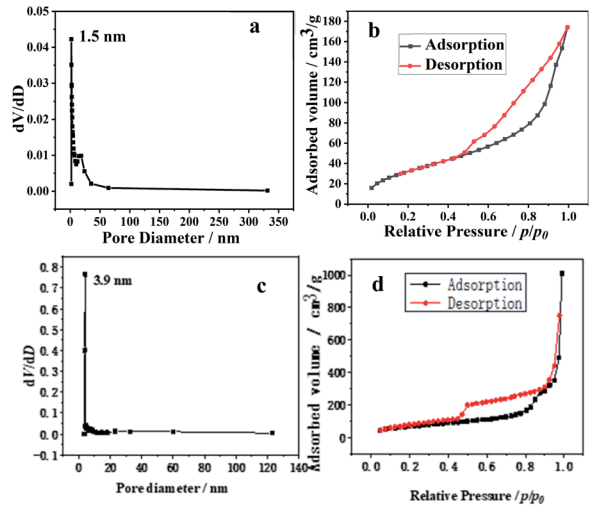

Fig. 2 The pore size distribution and isotherms of the hollow SiO_2 (a and b) and p-l-hSiO_2 (c and d) adsorbent.

Fig. 3a gives the XRD pattern of the synthesized hollow SiO_2 and p-l-hSiO_2 adsorbent. It can be seen that the XRD pattern exhibits an obvious broad diffraction peak around 23°, which is indexed to the scattering of amorphous SiO_2 (JCPDS 76-0933). Interestingly, the gotten p-l-hSiO_2 adsorbent presents multiple diffraction peaks and a broad back peak. The broad back peak around 23° is assigned to amorphous silica (JCPDS card no. 76-0933); the characteristic peak at 2 theta = 15.0° (001), 28.2° (100), 32.1° (101) and 41.9° (102) are consistent with the standard XRD data of Berndtite-2T SnS_2 (JCPDS card no. 23-0677).[28] This could be because the solubility of SnS_2 (ksp(SnS_2) = 10) is smaller than that of SnO_2 (ksp(SnO_2) = 398) and SnO_2 QDs can easily react with –SH group to form –S–Sn–S structure. As a result, several SiO_2–SH NSs are connected into peanut-like NSs with the assistance of the Sn–S bond, and the silica NSs changed to peanut-like NSs.

Fig. 4 presents the element composition of the p-l-hSiO_2 adsorbent determined by EDS analysis. It can be seen that it is made of Si, O, C, S and Sn elements and exhibits a S : Sn atomic ratio of about 86 : 1. According to the results of XRD, it can be seen that there is the characteristic peaks of SnS_2, indicating the atomic ratio of S : Sn should be 2 : 1. However, the S : Sn is 86 : 1 from EDS analysis, more than that in SnS_2. It may be some of –SH groups have not react with SnO_2, which indicates that there exists –S–Sn–S and –SH species. And this result is consistent with that of XRD analysis.

Fig. 5 schematically illustrates the formation of p-l-hSiO_2 adsorbent and their application in separating GST-tagged proteins. Firstly, the p-l-hSiO_2–SH NSs is synthesized by one-pot method. Then the prepared p-l-hSiO_2–SH NSs are modified with GSH molecule to afford p-l-hSiO_2–GSH NSs. Lastly, the p-l-hSiO_2–GSH NSs are used to separate the GST-tagged proteins from the *E. coli* lysate. In particular, the prepared p-l-hSiO_2 adsorbent can be purified the target proteins for several times.

Fig. 6 shows the SDS-PAGE of the GST-tagged GPX3 separated by p-l-hSiO_2 adsorbent from *E. coli* lysate without pretreatment. It can be seen that the prepared p-l-hSiO_2 adsorbent can separate specifically GST-tagged GPX3 (lane 1 in Fig. 6), and their binding capacity to the target proteins is 6.80 mg g^{-1}, which is higher than that of the report in ref. 29

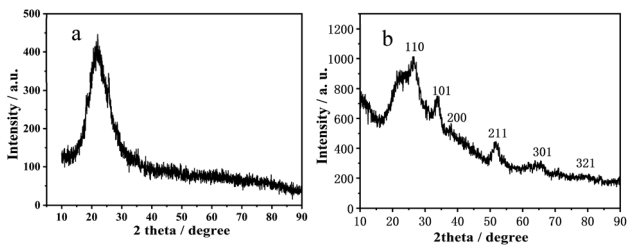

Fig. 3 XRD images of the synthesized the hollow SiO_2 (a) and p-l-hSiO_2 (b) adsorbent.

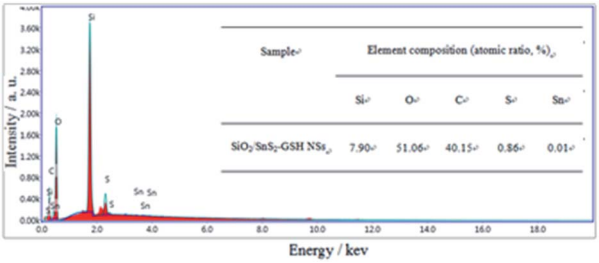

Fig. 4 EDS analysis of the p-l-hSiO$_2$ adsorbent.

indicates the good specificity and separation efficiency. In order to investigate the reused properties of the prepared p-l-hSiO$_2$ adsorbent, we separated GST-tagged GPX3 for three times by the same p-l-hSiO$_2$ adsorbent. As shown in Fig. 6 lane 2–4, the adsorbent exhibits specific selectivity to the target proteins extracted from *E. coli* lysate in three times reuse, and their binding capacity of GST-tagged GPX3 is 6.8 mg g^{-1}, 6.4 mg g^{-1} and 6.4 mg g^{-1}, respectively. Meanwhile, the content of GST-tagged GPX3 in 1 mL *E. coli* lysate is about 0.497 mg, and the content of target protein separated by p-l-hSiO$_2$ adsorbent from 1 mL *E. coli* lysate is about 0.448 mg, so the recovery of the target protein is about 90.1%. This indicates that the prepared p-l-hSiO$_2$ adsorbent can be well recycled after separating the GST-tagged GPX3.

Equilibrium studies are performed to determine the capacity and equilibrium constant of GST-tagged GPX3 protein adsorbed on p-l-hSiO$_2$ nanostructures. Langmuir model and Freundlich model are employed to show the adsorption relationship. The Langmuir (1) and Freundlich (2) equations are given.

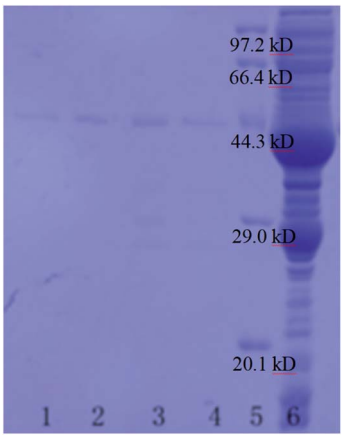

Fig. 6 The standard SDS-PAGE of the proteins separated by p-l-hSiO$_2$ adsorbent. Lane 1, GST-tagged GPX3 separated by prepared p-l-hSiO$_2$ adsorbent; lane 2–4, separation after three reuse of p-l-hSiO$_2$ adsorbent: lane 2: 1st separation, lane 3, 2nd separation, lane 4, 3rd separation; lane 5, Marker; lane 6, *E. coli* lysate.

$$\frac{C_e}{Q_e} = \frac{1}{Q_m} C_e + \frac{1}{bQ_m} \quad (1)$$

$$\ln Q_e = \frac{1}{n} \ln C_e + \ln k \quad (2)$$

where C_e (mg mL^{-1}) is the equilibrium concentration of GST-tagged GPX3 protein in *E. coli* lysate; Q_e (mg g^{-1}) is the adsorption capacity of GST-tagged GPX3 protein per gram of p-l-hSiO$_2$, and Q_m (mg g^{-1}) was the maximum adsorption capacity of p-l-hSiO$_2$; b (L mg^{-1}) was the Langmuir constant, k (mg g^{-1}) was the Freundlich isothermal constant, and $1/n$ was the degree

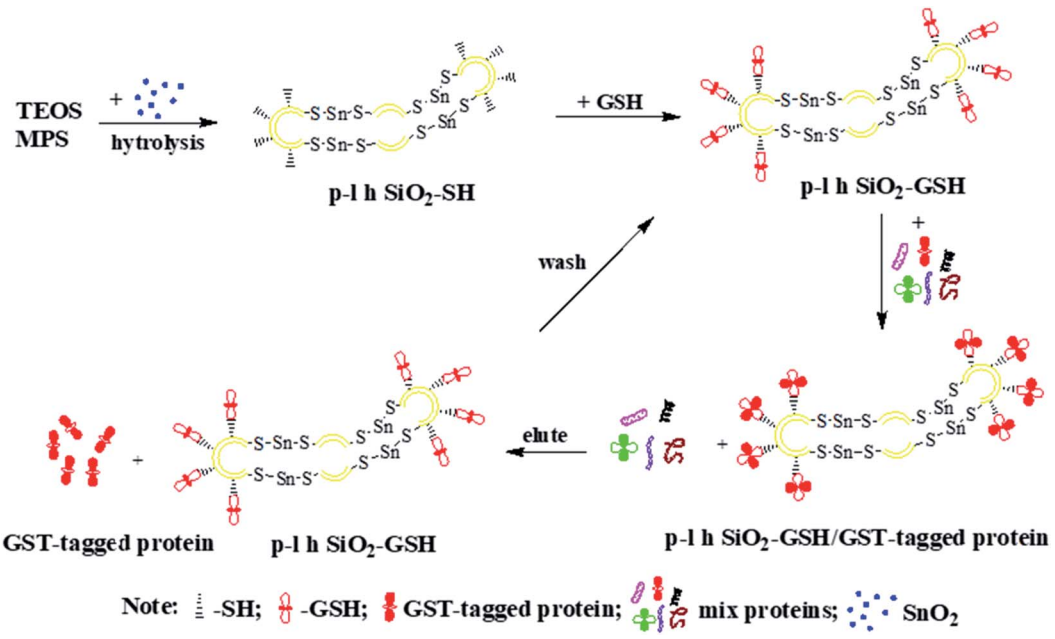

Fig. 5 Mechanism diagram of synthesis of p-l-hSiO$_2$ adsorbent and separation of GST-tagged protein.

of nonlinearity between protein concentration and adsorption capacity.[30]

Fig. 7 shows the plots of Langmuir (a) and Freundlich (b) isotherms. As can be seen from Fig. 7a, the regression coefficient of Langmuir model ($R^2 = 0.99$) is higher than that of Freundlich model ($R^2 = 0.10$), the Langmuir model is more suitable for the interpretation of experimental data. Meanwhile, the Q_m from Langmuir model was recorded as 6.73 mg g^{-1}, which is consistent with the results of adsorption experiment (6.8 mg g^{-1}). The results showed that p-l-hSiO$_2$ adsorption exhibited a good separation ability for GST-tagged GPX3.

Kinetic studies are usually employed to analyze the adsorption time required for reaction equilibrium. There are two kinetic models: pseudo 1st (3) and pseudo 2nd (4) models, and the kinetic equations are as follows:

$$\ln(Q_e - Q_t) = -k_1 t + \ln Q_e \quad (3)$$

$$t/Q_t = \frac{t}{Q_e} + \frac{1}{k_2 Q_e^2} \quad (4)$$

where Q_e (mg g^{-1}) and Q_t (mg g^{-1}) are the amounts of GST-tagged GPX3 protein adsorbed per gram of p-l-hSiO$_2$ at equilibrium state and at time t, respectively. k_1 (min^{-1}) and k_2 (g (mg min)$^{-1}$) are the rate constants of pseudo 1st and 2nd models respectively.[31]

Fig. 8a and b are kinetic analysis of GST-tagged GPX3 adsorbed by p-l-hSiO$_2$ adsorbent. The R^2 from the pseudo 1st was 0.95, while that from the pseudo 2nd was $R^2 = 0.99$, which indicates that the adsorption data is in better agreement with the pseudo 2nd kinetic model. At the same time, the Q_e value of 6.66 mg g^{-1} calculated by the pseudo 2nd model is consistent with the experimental Q_e value of 6.80 mg g^{-1}. This indicates that synthesized p-l-hSiO$_2$ adsorbent can be a promising regenerated adsorbent for GST-tagged proteins.

Experimental

Materials

3-Mercaptopropyltrimethoxysilane (MPS) was purchased from Alfa-Aesar (USA, AR, 95.0%). Tetraethyl orthosilicate (TEOS) was commercially obtained from Tianjin Fuchen Chemicals (Tianjin, China, AR, 98.0%). Hexadecyltrimethylammonium chloride (CTAC) was purchased from Sinopharm Chemicals (Beijing, China, AR, 99.0%).

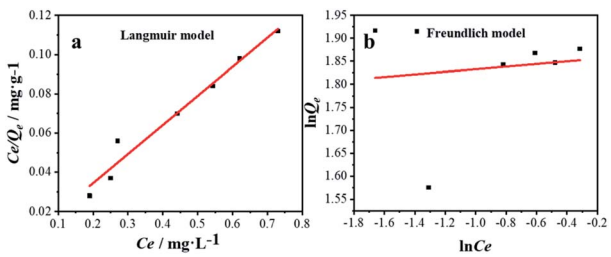

Fig. 7 The Langmuir model (a) and Freundlich model (b), of p-l-hSiO$_2$ adsorbent on GST-tagged GPX3.

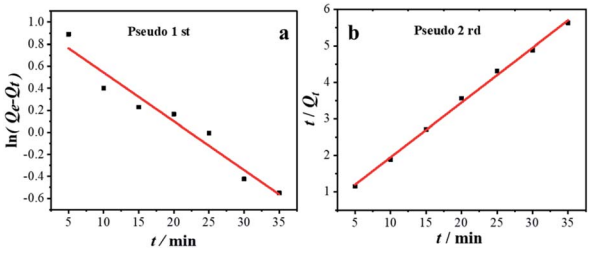

Fig. 8 The pseudo 1st (a) and pseudo 2nd (b) of p-l-hSiO$_2$ adsorbent on GST-tagged GPX3.

Synthesis of the p-l-hSiO$_2$ adsorbent

SnO$_2$ quantum dots (QDs) are prepared by a hydrothermal process.[32] Briefly, 0.2 μmol SnO$_2$ QDs, 0.09 g CTAC, 7.0 mL ethanol, and 2.75 mL TEA are sequentially dispersed in 42.5 mL H$_2$O. The resultant solution is heated to 60 °C with a water bath, followed by the slow addition of 3.5 mL TEOS and 0.35 mL MPS. The mixed solution is kept at 60 °C for 5 h and then transferred into a Teflon-lined stainless-steel autoclave and heated at 110 °C for 48 h. Upon completion of heating, the solution is cooled, filtered and washed to obtain the p-l-hSiO$_2$–SH NSs. Then 6 mL p-l-hSiO$_2$–SH NSs (0.59 g mL^{-1}) are washed with PBS (0.01 mol L; pH = 7.4) for several times. The washed p-l-hSiO$_2$–SH NPs are placed in 30 mL GSH solution (16.0 mg mL^{-1}), and the resultant mixed solution is oscillated at 37 °C for 24 h (120 rpm). Upon completion of oscillation, the mixed solution is centrifuged and washed to afford p-l-hSiO$_2$ adsorbent.

Affinity separation of GST-tagged proteins

The mixed proteins are collected from *E. coli* lysate. Then 160 μL p-l-hSiO$_2$ adsorbent (0.07 g mL^{-1}) is washed with PBS and then directly introduces into 1.0 mL of cell lysate mixture. The mixed solution is incubated for 2 h at 4 °C to allow the p-l-hSiO$_2$ adsorbent to capture the GST-tagged glutathione peroxidase 3 (GST-tagged GPX3). Subsequently, the captured GST-tagged proteins are eluted with 300 μL GSH solution (50 mmol L^{-1}) to disassociate the GST-tagged proteins from the surfaces of p-l-hSiO$_2$ adsorbent. The p-l-hSiO$_2$ adsorbent can be reused for several times if desired.

Adsorption thermodynamics and adsorption kinetics

Then the adsorption thermodynamics and adsorption kinetics of p-l-hSiO$_2$ adsorbent on GST-tagged GPX3 are studied. Briefly, different amounts (0.01 g, 0.015 g, 0.02 g, 0.025 g, 0.03 g, 0.035 g and 0.04 g) of p-l-hSiO$_2$ are added into 1.5 mL *E. coli* lysate by incubated at 4 °C for 2 h. Subsequently, the p-l-hSiO$_2$ samples captured GST-tagged GPX3 adre washed six times by PBS (0.01 M, pH 7.4). After washing, these precipitates are eluted by 100 μL glutathione (50 mM), and the concentration of gotten proteins in supernatant are analyzed by an ultraviolet-visible light spectrophotometer at 280 nm.

In order to further study the kinetics of p-l-hSiO$_2$ adsorption on GST-tagged GPX3, ten p-l-hSiO$_2$ samples are weighed in parallel (0.02 g each). Then 1.5 mL of *E. coli* lysate are added into

these ten p-l-hSiO_2 samples, respectively, and incubated at 4 °C at different time intervals (5, 10, 15, 20, 25, 30, 35, 40 and 60 min). After centrifugation, these precipitates are washed by PBS (0.01 M, pH 7.4) and eluted by 100 μL glutathione (50 mM). And the concentration of gotten GST-tagged GPX3 proteins in supernatant are analyzed by the ultraviolet-visible light spectrophotometer at 280 nm.

Characterization

The morphology and composition of the p-l-hSiO_2 adsorbent is analyzed by scanning electron microscopy (SEM, JSM 5600LV, Japan), X-ray diffraction (XRD, X′ Pert, Holland), energy dispersive spectrometric (EDS, JSM 5600LV, Japan) and transmission electron microscopy (TEM, JEM-2010, Japan). The surface area is measured by the Brunauer–Emmett–Teller method (BET, QUADRASORB, American). Moreover, the separated GST-tagged proteins are detected by sodium dodecylsulfate polyacrylamide gel electrophoresis (SDS-PAGE, Power PAC 300; China), and the binding concentration of the proteins is determined with an ultraviolet-visible light spectrophotometer at 280 nm (Nanodrop 2000c; USA).

Conclusions

Peanut-like silica hollow NSs functionalized by thiol group are prepared by a facile hydrothermal route. The resultant SiO_2–SH NSs are further modified by GSH to afford p-l-hSiO_2 adsorbent for the affinity separation of GST-tagged proteins. They exhibit specific adsorption, high binding capacity, and good reused performance, which makes it possible to apply them to the visual separation and purification of GST-tagged proteins.

Conflicts of interest

The authors declares no potential conflicts of interest with respect to the research, authorship, and/or publication of this article. Meanwhile, the author's order has been sorted out according to the author's contribution to this article.

Acknowledgements

The authors acknowledge the financial support provides by the fellowship of China Postdoctoral Science Foundation (2021M690913); Key Scientific Research Project of Henan Province (21A150012); Henan University (in the name of "Innovation and Entrepreneurship Training Program for College Student", 20211015005, 20211015006, 20211015004, 20211015007); Natural Science Foundation of Shenzhen (JCYJ20210324093211030) and Interdisciplinary Research for First-class Discipline Construction Project of Henan University (2019YLXKJC04).

Notes and references

1 K. Richare, B. Chris, R. Lucy, *et al.* Enrichment of low molecular weight serum proteins using acetonitrile precipitat ion form assspectrometry based proteomic analysis, *Rapid Commun. Mass Spectrom.*, 2008, **20**, 3255–3260.

2 Y. D. Luo, X. Q. Huang and W. L. McKeehan, High yield, purity and activity of soluble recombinant Bacteroides thetaiotaomicron GST-heparinase I from Escherichia coli, *Arch. Biochem. Biophys.*, 2007, **460**, 17–24.

3 Y. B. Yin, G. M. Wei, X. Y. Zou and Y. B. Zhao, Functionalized hollow silica nanospheres for His-tagged protein purification, *Sens. Actuators, B*, 2015, **209**, 701–705.

4 J. Zheng, C. J. Ma, Y. F. Sun, M. R. Pan, L. Li, X. J. Hu and W. L. Yang, Maltodextrin-modified magnetic microspheres for selective enrichment of maltose binding Proteins, *ACS Appl. Mater. Interfaces*, 2014, **6**, 3568–3574.

5 X. Y. Zou, Y. Zhang, J. Q. Yuan, Z. B. Wang, R. Zeng, K. Li, Y. B. Zhao and Z. J. Zhang, Porous nano-adsorbent with dual functional groups for selective binding proteins with a low detection limit, *RSC Adv.*, 2020, **10**, 23270–23275.

6 T. Ding, J. Z. Xu, J. Z. Li, C. Y. Shen, B. Wu, H. L. Chen and S. J. Li, Determination of melamine residue in plant origin protein powders using high performance liquid chromatography-diode array detection and high performance liquid chromatography-electrospray ionization tandem mass spectrometry, *Chin. J. Chromatogr.*, 2008, **26**, 6–9.

7 E. Maltas, M. Ozmen, H. C. Vural, *et al.* Immobilization of albumin on magnetite nanoparticles, *Mater. Lett.*, 2011, **65**, 3499–3501.

8 M. Vinoba, M. Bhagiyalakshmi, S. K. Jeong, Y. I. Yoon and S. C. Nam, Capture and sequestration of CO_2 by human carbonic anhydrase covalently immobilized onto amine-functionalized SBA-15, *J. Phys. Chem. C*, 2011, **115**, 20209–20216.

9 S. F. Tian, X. Y. Zou, H. T. Lu, J. Y. He, Y. B. Zhao and J. Y. Guo, Synthesis of nanometer hollow silica composite microspheres for affinity separation of protein, *Chin. J. Inorg. Chem.*, 2015, **31**, 1329–1334.

10 M. Zhang, Y. P. Wu, X. Z. Feng and X. W. He, Fabrication of mesoporous silica-coated CNTs and application in size-selective protein separation, *J. Mater. Chem.*, 2010, **126**, 5835–5842.

11 C. J. Xu, Z. H. Guo, R. K Zheng, H. W. Gu, H. Liu, B. Xu, K. M. Xu and X. X. Zhang, Dopamine as a robust anchor to immobilize functional molecules on the iron oxide shell of magnetic nanoparticles, *J. Am. Chem. Soc.*, 2004, **126**, 9938–9939.

12 X. Y. Zou, K. Li, Y. B. Yin, Y. B. Zhao, Y. Zhang, B. J. Li, S. S. Yao and C. P. Song, Synthesis of petal-like ferric oxide/cysteine architectures and their application in affinity separation of proteins, *Mater. Sci. Eng., C*, 2014, **34**, 468–473.

13 X. Y. Zou, K. Li, Y. B. Zhao, Y. Zhang, B. J. Li and C. P. Song, Ferroferric oxide/L-cysteine magnetic nanospheres for capturing histidine-tagged proteins, *J. Mater. Chem. B*, 2013, **1**, 5108–5113.

14 Y. Wang, G. Wang, Y. Xiao, Y. L. Yang and R. K. Tang, York-shell nanostructured Fe_3O_4@$NiSiO_3$ for selective affinity and

magnetic separation of His-tagged proteins, *ACS Appl. Mater. Interfaces*, 2014, **6**, 19092–19099.
15 T. C. Lu, J. Sun, X. Q. Dong, X. S. Chen, Y. Wang and X. B. Jing, *Sci. China, Ser. B: Chem.*, 2009, **39**, 1598–1602.
16 M. Rembutsu, M. P. M. Soutar, L. V. Aalten, R. Gourlay, J. Hastie, H. Mclauchlan, N. A. Morrice, A. R. Cole and C. Sutherland, *Biochem*, 2008, **47**, 2153–2161.
17 X. Y. Zou, F. B. Yang, X. Sun, M. M. Qin, Y. B. Zhao and Z. J. Zhang, *Nanoscale Res. Lett.*, 2018, **13**, 165–172.
18 J. J. Zhu, L. Yang, L. Yang, C. Chen and Y. L. Cui, *Chin. J. Biotechnol.*, 2009, **25**, 1254–1260.
19 F. Xu, J. H. Geiger, G. L. Baker and M. L. Bruening, *Langmuir*, 2011, **27**, 3106–3112.
20 N. Cao, X. Y. Zou, Y. Q. Huang and Y. B. Zhao, *Mater. Lett.*, 2015, **144**, 161–164.
21 S. K. Sahu, A. Chakrabarty, D. Bhattacharya, S. K. Ghosh and P. J. Pramanik, *J. Nanopart. Res.*, 2011, **13**, 2475–2484.
22 D. R. Bae, S. J. Lee, S. W. Han, J. M. Lim, D. M. Kang and J. H. Jung, *Chem. Mater.*, 2008, **20**, 3809–3813.
23 B. B. Chen, H. Liu, C. Z. Huang, J. Ling and J. Wang, *New J. Chem.*, 2015, **39**, 1295–1300.
24 B. J. Li, X. Y. Zou, Y. B. Zhao, L. Sun and S. L. Li, *Mater. Sci. Eng., C*, 2013, **33**, 2595–2600.
25 S. B. Tural, B. Sopac, N. Özkan, S. A. Demir and M. Volkan, *J. Phys. Chem. Solids*, 2011, **72**, 968–973.
26 J. Y. Hu, Q. Li, X. K. Zhong and W. Kang, *Prog. Org. Coat.*, 2008, **63**, 13–17.
27 J. Jin, Z. P. Zhang, Y. Li, X. B. Lu, L. D. Wu and J. P. Chen, *Anal. Chim. Acta*, 2011, **693**, 54–61.
28 Y. H. Fan, Q. Li, G. X. Liu and J. X. Wang, *Chin. J. Inorg. Chem.*, 2014, **30**, 627–632.
29 X. Y. Zou, L. L. Li, H. T. Lu, Y. Y. Zhang, Y. B. Zhao, Y. Zhang and Q. H. Guo, *Process Biochem.*, 2016, **51**, 804–808.
30 X. Y. Zou, Y. B. Yin, Y. B. Zhao, D. Y. Chen and S. Dong, Synthesis of ferriferous oxide/L-cysteine magnetic microspheres and their adsorption capacity for Pb (II) ions, *Mater. Lett.*, 2015, **150**, 59–61.
31 X. Y. Zou, Y. B. Zhao and Z. J. Zhang, Preparation of hydroxyapatite nanostructures with different morphologiesand adsorption behavior on seven heavy metals ions, *J. Contam. Hydrol.*, 2019, **226**, 103538–103544.
32 Z. J. Li, W. Z. Shen, Z. Wang, X. Xiang, X. T. Zu, Q. M. Wei and L. Wang, *J. Sol-Gel Sci. Technol.*, 2009, **49**, 196–201.